

We are IntechOpen, the world's leading publisher of Open Access books Built by scientists, for scientists

6,900

Open access books available

185,000

International authors and editors

200M

Downloads

Our authors are among the

154

Countries delivered to

TOP 1%

most cited scientists

12.2%

Contributors from top 500 universities



WEB OF SCIENCE™

Selection of our books indexed in the Book Citation Index
in Web of Science™ Core Collection (BKCI)

Interested in publishing with us?
Contact book.department@intechopen.com

Numbers displayed above are based on latest data collected.
For more information visit www.intechopen.com



Reduced Graphene Oxide–Based Microsupercapacitors

Zhi Jiang, Yang Wang and Cheng Yang

Additional information is available at the end of the chapter

<http://dx.doi.org/10.5772/67433>

Abstract

Recent development in miniaturized electronic devices has been boosting the demand for power sources that are sufficiently thin, flexible/bendable, and even tailorable and can potentially be integrated in a package with other electronic components. Reduced graphene oxide can be a promising electrode material for miniaturized microsupercapacitors due to their excellent electrical conductivity, high surface-to-volume ratio, outstanding intrinsic electrochemical double-layer capacitance, and facile production in large scale and low cost. Therefore, the routes to produce high-quality reduced graphene oxide as electrode materials, along with the typical fabrication techniques for miniaturized electrodes, are deliberately discussed in this chapter. Furthermore, breakthroughs in the area of the advanced packaging technology, deciding the electrochemical performance and stability of these miniaturized microsupercapacitors, are highlighted. Lastly, a summary of the overall electrochemical properties and current development of the reported devices is presented progressively to provide insights into the development of novel miniaturized energy storage technologies.

Keywords: reduced graphene oxide, miniaturized supercapacitor, flexible/bendable supercapacitor, laser, packaging technique

1. Introduction

The recent boom in portable electronic devices has raised great demand for miniaturized, flexible/bendable, and even tailorable energy storage devices, which can be directly integrated with a series of electronic devices, to provide unprecedented high-performance functionalities [1, 2]. Currently, the thickness of commercial miniaturized supercapacitors is still faced with great challenges to be further shrunk with the size to the level of surface mountable resistors and ceramic capacitors, which has hindered their application in integrated electronic devices. Microsupercapacitors (MSCs) with a thickness of 10–100 μm can fulfill the above-mentioned

requirements because of their excellent rate capability, high power density, and long lifetime [3–5]. Also, ultrathin MSCs with polymer substrates showed great flexibility, which can make full use of interstitial spaces among components in an integrated system [2, 6].

This chapter reviews the recent progress of fabrication strategies for reduced graphene oxide (r-GO) and exemplifies some very promising r-GO-based MSC technologies; besides, it shows the breakthroughs in packaging techniques for these novel devices. It will provide insights to the development of novel miniaturized energy storage technologies.

2. Typical fabrication methods of high-quality r-GO as the electrode material

Graphite oxide consists of layered graphene oxide (GO) nanosheets that contain many oxygen functional groups, such as hydroxyl, epoxide, carbonyl, and carboxyl groups, which promote the formation of few-layer GO nanosheets [7]. However, these functional groups also destroy the planar sp^2 carbons of graphite by converting them into sp^3 carbons and alter van der Waals interactions between these layers. The structural changes bring about two problems of GO nanosheets for supercapacitors: one is that the electrical conductivity of GO is much lower than that of graphene and the other is the strong hydrophilicity of GO nanosheets. Therefore, GO cannot be used as an electrode material for supercapacitors without further treatments. Notably, the electrical conductivity of r-GO can be increased close to the level of graphene, and the specific capacitance of r-GO has been found to be significantly higher than that of GO. Herein, the reduction routines of GO to r-GO are systematically introduced.

2.1. Chemical reduction of GO

The chemical reduction of GO route involves reducing agents to eliminate most of oxygen-containing functional groups of GO nanosheets and partially restore the π -electron conjugation within the aromatic system of graphite [8]. The reducing agents can be categorized into toxic ones and environment-friendly ones. Though toxic reducing agents, such as hydrazine, hydrazine monohydrate, dimethylhydrazine, sodium borohydride, hydroquinone, and hydroxylamine, have been shown to efficiently reduce GO into r-GO [9–13], they are not suitable for the future large-scale fabrication of electrode materials due to their damages to the environment. Therefore, environmental friendly reducing agents, such as amino acids and ammonia, have attracted more attention. Pham et al. developed a green and facile approach to produce r-GO by using an environmental friendly reagent, namely L-glutathione as a reducing agent, under mild condition in aqueous solution [14]. The L-glutathione-r-GO could be dispersed in both distilled water and some polar aprotic solvents, including Dimethylformamide (DMF), Dimethyl sulfoxide (DMSO), and Tetrahydrofuran (THF) with simple ultrasonication, because the oxidized product of L-glutathione could play an important role as a capping agent in the stabilization of r-GO. As this chemical reduction process of GO could produce r-GO in a bulk quantity in a relatively short time and mild experimental conditions without any environmentally hazardous chemicals, it offers excellent flexibility for various potential applications not only in electronic devices but also in biocompatible

materials. Chen et al. prepared r-GO through the reduction of GO employing L-cysteine as the reductant under a mild reaction condition [15]. During this chemical reduction process, the thiol group of L-cysteine released protons, commonly owning high-binding affinity to the oxygen-containing groups of GO, such as hydroxyl and epoxide groups, to form water molecules, which was similar to L-glutathione. Furthermore, the electrical conductivity of r-GO produced in this way increased by about 10^6 times in comparison to that of GO.

Jiang et al. reported an ammonia-assisted hydrothermal method to obtain N-doped r-GO by simultaneous N-doping and reduction of GO [16]. The effects of hydrothermal temperature on the surface chemistry and the structure of N-doped rGO were investigated. Their results showed that N doping was accompanied by the reduction of GO with a decrease in oxygen levels from 34.8% in GO down to 8.5% in N-doped r-GO. Meanwhile, electrochemical measurements demonstrated that the N-doped product showed a higher capacitive performance than that of pure graphene, and a maximum specific capacitance of 144.6 F/g could be obtained by the pseudocapacitive effect from the N-doping. Li et al. obtained bulk quantities of N-doped r-GO through thermal annealing of GO in ammonia [17]. X-ray photoelectron spectroscopy (XPS) study of GO annealed at various reaction temperatures revealed that N-doping occurred at a temperature as low as 300°C while the highest doping level of about 5% N was achieved at 500°C. Oxygen groups in GO were found responsible for reactions with NH_3 and C-N bond formation, and r-GO obtained by the annealing of GO in NH_3 exhibited higher electrical conductivity than that of r-GO by the annealing GO in H_2 .

R-GO obtained by the chemical reduction method showed good electrical conductivity, high specific capacitance value, and excellent dispersibility in different organic solvents. However, the totally removal of oxygen functionalities from the surface of GO nanosheets is impossible by using chemical reducing agents. Therefore, other reduction methods of GO for the large-scale production of high-quality r-GO have been proposed.

2.2. Thermal reduction of GO

Thermal reduction of GO is one of the most well-known methods for the removal of oxygen-containing functional groups [18]. In this type of reduction process, most of oxygen functionalities were transformed into water, carbon dioxide, and carbon monoxide. Usually, the GO sample is placed in a specific furnace filled with inert gas environment and then heated to a relatively high temperature. During the reduction process, reductive gases are generated to reduce GO and to expand their layers at the same time.

Schniepp et al. obtained r-GO by annealing GO nanosheets in a closed quartz tube at 1050°C under the protection of argon atmosphere for 10 min, and the carbon content in the final r-GO product increased with the rise of the annealing temperature [19]. They fabricated polymer nanocomposites with stacks of these r-GO nanosheets as the filler, and the as-fabricated polymer showed outstanding thermal, mechanical, and electrical properties. Such functionalized r-GO nanosheets can provide even further benefits, not only for structural property enhancements at lower filler contents, but also for the development of new materials such as electrically conducting polymers, conductive inks, and supercapacitors. Vallés et al. reported a considerable recovery of the sp^2 network structure of r-GO by a relatively simple thermal

treatment at 700°C under argon or hydrogen atmosphere [20]. The as-fabricated r-GO paper exhibited an excellent electrical conductivity as high as 8100 S/m, which was five orders of magnitude higher than that of initial GO paper, and also much higher than that of r-GO paper by a chemical reduction method. Moreover, this gentle and direct thermal reduction method allowed r-GO paper to remain the good structural integrity and mechanical flexibility of the initial GO paper, overcoming problems of brittleness typically encountered in the annealing process. Mattevi et al. reported that the effect of annealing GO at 700°C or above was equivalent to the chemical reduction of GO via hydrazine monohydrate at 80°C followed by heating at 200°C [21]. For fully reduced GO nanosheets, they found the oxygen content was about 8% with the ratio of C to O equaling to 12.5:1 and the sp^2 concentration being 80%, and they demonstrated that the presence of residual oxygen with only 8% content significantly hampered the carrier transport among the graphitic domains.

The thermal reduction of GO is a direct, cost-effective, and environmentally friendly route for the fabrication of high-quality r-GO. However, it usually needs a high temperature to obtain r-GO with a high electrical conductivity, and the experimental set-up is very complicated, all of which have hindered its further application.

2.3. Electrochemical reduction of GO

The routine of electrochemical reduction of GO nanosheets was newly proposed for the fabrication of high-quality r-GO whose defect concentration is almost negligible. Electrochemically reduced GO (Er-GO) nanosheets are contaminant-free and of high electrical conductivity, which makes them suitable for applications in the areas of supercapacitor devices, touch screens, and flexible electronics.

Li et al. firstly reported a fiber-shaped solid electrochemical capacitor based on Er-GO [22]. The typical fiber-shaped electrode can be prepared by electrochemically reducing GO on an Au wire with a diameter of 100 μ m in 3-mg/mL GO aqueous suspension containing 0.1-M lithium perchlorate ($LiClO_4$) at an applied potential of about 1.2 V (vs. saturated calomel electrode, SCE) for 10 s, and it exhibited high specific capacitance and rate capability, long cycling life, and also attractive mechanical flexibility. Yang et al. demonstrated the application of Er-GO as supercapacitor electrodes by reducing GO in a convenient, cost-effective, and eco-friendly electrochemical way [23]. During the electrochemical reduction process, p-conjugated structure in graphene was almost completely repaired by removing electrochemically unstable oxygen groups, yielding improved electron transfer kinetics and capacitive properties of Er-GO. At the same time, residual oxygen groups on Er-GO nanosheets were very stable and reversible in capacitive performance providing additional faradic pseudocapacitance without damaging their electronic properties. As a result, the Er-GO exhibited a specific capacitance of as high as 223.6 F/g at 5 mV/s, showing a promising potential as an electrode material for supercapacitors.

Chen et al. reported a general method for the fabrication of three-dimensional (3D) porous Er-GO-based composite materials [24]. First, 3D porous Er-GO was prepared electrochemically by reducing a concentrated GO aqueous solution containing 0.15-M $LiClO_4$ as shown in **Figure 1a**. The cyclic voltammogram of a copper foil electrode in the GO and $LiClO_4$ electrolyte

at the scan rate of 50 mV/s was shown in **Figure 1b**, and the redox peak appeared at about -1.15 V. The X-Ray diffraction (XRD) pattern of Er-GO film obtained by reducing 3-mg/mL GO solution at a potential of 1.15 V for 300 s, confirmed that most of electrochemically unstable oxygen groups were removed from initial GO film. The as-fabricated Er-GO-based paper electrode, prepared by electrochemically reducing 3-mg/mL GO at a potential of 1.15 V for 600 s, was shown in **Figure 1d**, and the Er-GO-based paper electrode exhibited a 3D porous structure, which was good for ion and electron transportation during the charge/discharge process. Furthermore, by the growth of polyaniline layer on 3D Er-GO paper electrodes, a high specific capacitance of 716 F/g at 0.47 A/g was achieved. Sheng et al. reported an electrochemical double-layer capacitor based on 3D interpenetrating r-GO electrodes fabricated by the electrochemical reduction of GO [25]. At 120 Hz, the Er-GO-based MSCs exhibited a phase angle of -84° , a specific capacitance of 283 mF/cm², and a resistor-capacitor (RC) time constant of 1.35 ms, making it capable of replacing activated carbon-based MSCs for AC-line filtering.

The electrochemical reduction of GO process is very fast and avoids the use of any harmful chemical reducing agents, which means that there is no need for further purification of Er-GO [26].

2.4. Laser reduction of GO

Laser reduction of GO routine uses laser as the major energy source to obtain porous r-GO nanosheets without the need for any additional chemical agents; and it leaves abundant defects in r-GO nanosheets, which can highly improve the electrochemical characteristic of r-GO [27–29]. Except from the reduction function, laser with a higher energy level can selectively remove GO/r-GO nanosheets without any damage to substrates due to the instant heating and cooling feature, which can make it possible for graphical electrodes [27, 30].

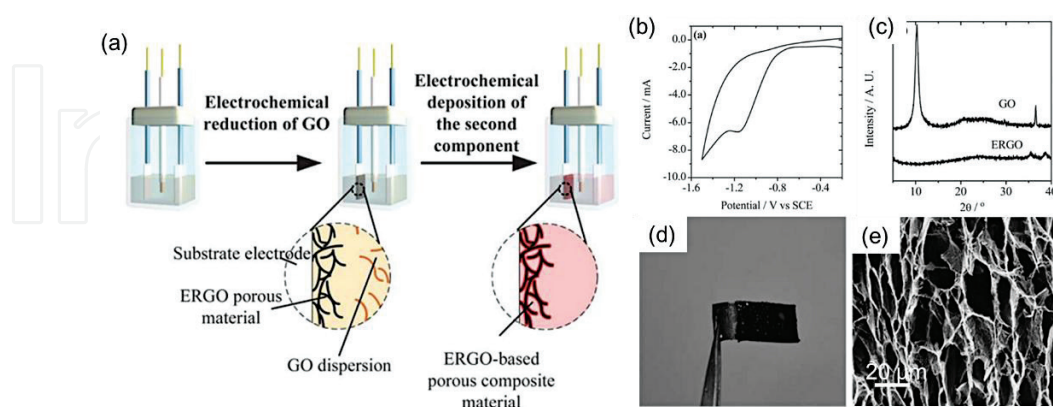


Figure 1. (a) Schematic illustration of the preparation method for Er-GO-based composite materials, (b) cyclic voltammogram of a copper foil electrode in 3-mg/mL GO aqueous solution containing 0.15-M LiClO₄ at a scanning rate of 50 mV/s, (c) XRD patterns of GO film and as-prepared wet Er-GO porous material by reducing 3-mg/mL GO solution at a potential of 1.15 V for 300 s, (d) optical image of Er-GO paper electrode prepared by electrochemically reducing 3 mg/mL GO at a potential of 1.15 V for 600 s. (e) SEM image of lyophilized Er-GO paper (Reproduced with permission from Ref. [24]).

Abdelsayed et al. reported a facile laser reduction method for the preparation of r-GO from GO [31]. They obtained few-layer r-GO nanosheets in water under ambient conditions without the use of any chemical reducing agent indicated by changes in the color of GO solutions, as shown in **Figure 2a**. Furthermore, XRD results of the products after different irradiation time confirmed that only 10-min irradiation of the 532-nm laser could totally reduce GO into r-GO. By this mild reduction treatment in water, the few-layer character of GO nanosheets was perfectly preserved in the final products with a thickness of 0.99 nm as shown in **Figure 2b** and **c**.

Sokolov et al. obtained r-GO via continuous-wave (532 nm) and pulsed (532 and 355 nm) laser irradiation of GO [32]. They investigated the graphene degree of r-GO with different laser power and background gas and fabricated micro-sized defects in r-GO film using laser with a higher energy, indicating laser could be an effective technique for reducing r-GO with high spatial resolution and patterning feature. Many attentions have been paid to the mechanisms of laser reduction and ablation of GO, and most of them focused on the interaction among electron, photo, exciton, and ions [32–34]. When GO nanosheets are exposed to a laser beam, deoxygenation reaction is triggered instantaneously via both photochemical and photothermal reduction pathways. Though electron-lattice temperature equilibration occurs on the picosecond time scale, strain associated with the oxygen in GO nanosheets can lead to exciton self-trapping, hole localization, and subsequent material removal, as indicated by the release of CO, CO₂,

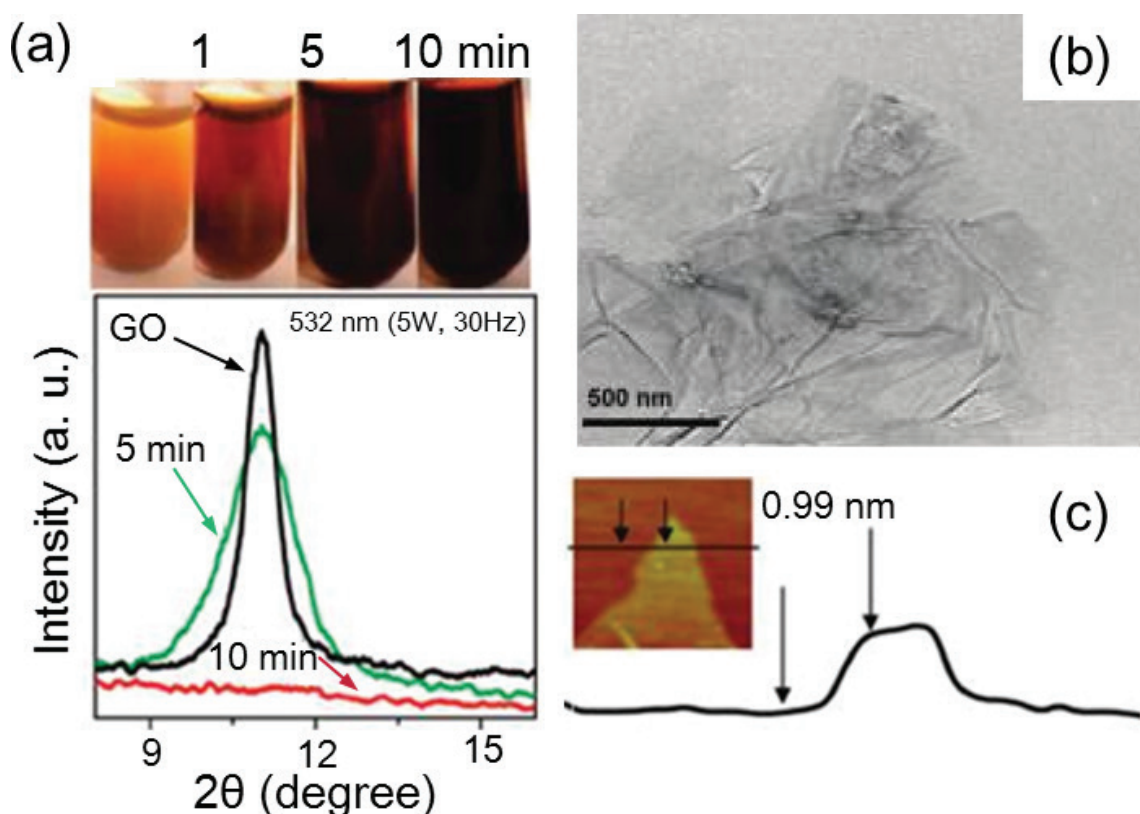


Figure 2. (a) Digital photographs displaying the changes in the color of the original GO solution (0 min) after irradiated with the 532-nm laser for 1, 5, and 10 min and the corresponding XRD results, (b) TEM images of r-GO nanosheets prepared by the 532-nm laser irradiation to the aqueous GO solution for 10 min, (c) AFM image and cross-sectional analysis of the r-GO nanosheets (Reproduced with permission from Ref. [31]).

and H_2O from GO nanosheets by laser irradiation [33]. During the ablation process of GO/r-GO nanosheets by laser, the release of high mass carbon cluster ions had been observed during photon- and low-energy electron-stimulated desorption, which can be deposited on the surface of r-GO nanosheets and served as seeds for growth of larger graphene particles or nanosheets [31].

Gao et al. demonstrated the scalable fabrication of an all-carbon monolithic supercapacitor by laser reduction and patterning of GO films [35]. They patterned both in-plane and sandwiched structured electrodes consisting of r-GO nanosheets with micrometer resolution, between which GO served as a solid-state electrolyte. The substantial amounts of trapped water in GO nanosheets made them simultaneously an excellent ionic conductor and an electrical insulator, allowing them to serve as both an electrolyte and an electrode separator with the ionic transport characteristics. The resulting microsupercapacitor devices showed an excellent cyclic stability and energy storage capacities as compared to the existing thin-film supercapacitors. El-Kady et al. used a standard LightScribe DVD optical drive to directly reduce GO films into r-GO by laser, and the as-fabricated r-GO-based films were mechanically robust and showed high electrical conductivity (1738 S/cm) and specific surface area ($1520 \text{ m}^2/\text{g}$) [36]. The r-GO-based supercapacitor exhibited a high energy density of as high as 1.36 mWh/cm^3 , which was approximately two times higher than that of the commercial activated carbon-based electrochemical capacitors (AC-EC). Moreover, a power density of about 20 W/cm^3 can be achieved, which was 20 times higher than that of the AC-EC and three orders of magnitude higher than that of the 500-mAh thin-film lithium battery.

Though laser reduction of GO cannot achieve mass production of r-GO, combined with film technology, r-GO fabricated via laser-reducing GO nanosheets is a promising electrode material for flexible, ultrathin, and binder-free microsupercapacitors and other electronic devices, such as sensors, displays, and batteries.

3. Recent progress of r-GO-based miniaturized microsupercapacitors

Rapid developments in semiconductor devices, low-power integrated circuits, and packaging technology are accelerating the reduction in the size and volume of current electronic devices, especially portable mobile communication equipment, implantable medical devices, and active radio frequency identification (RFID) tags. It makes rechargeable high-performance miniaturized energy storage devices become an urgent need [37]. R-GO-based miniaturized MSCs exhibit excellent rate capability, high power density, long lifetime, and good 3D micro-integration capability with other components, showing a promising perspective for the use as miniaturized energy storage devices. Here, some of recent representative works in the area of r-GO-based miniaturized MSCs are progressively introduced.

El-Kady et al. demonstrated scalable fabrication of high-power graphene microsupercapacitors for on-chip energy storage by direct laser writing on graphite oxide films using a standard LightScribe DVD burner [38]. **Figure 3a** shows the features of r-GO-based MSCs on a chip, and **Figure 3b** shows the morphological change of GO films after direct laser irradiation. The as-fabricated r-GO-based MSCs showed an excellent electrochemical performance and good flexibility on a flexible polymer substrate. Furthermore, the adaptability of r-GO-based MSCs for

serial/parallel combinations was demonstrated by connecting four devices together both in series and in parallel configurations, as shown in **Figure 3c** and **d**. The tandem MSCs exhibited a very good control over the operating voltage window and capacity, thus enabling them to be considered for practical applications. **Figure 3e** shows a Ragone plot comparing the performance characteristics of r-GO-based MSCs with different energy-storage devices designed for high power microelectronics. Remarkably, compared with activated carbon-based MSCs, r-GO-based MSCs exhibited three times higher energy and about 200 times higher power density. Furthermore, r-GO-based MSCs demonstrated power densities comparable to those of the aluminum electrolytic capacitor while providing more than three orders of magnitude higher energy density. This superior energy and power performances of the r-GO-based MSCs should enable them to compete with microbatteries and electrolytic capacitors in a variety of applications.

Xie et al. developed device-level tailorable gel-based MSCs with symmetric electrodes prepared by electrochemically reducing and depositing GO on a nickel nanocone array (NCA) current collector using a unique packaging method [39]. **Figure 4a** shows the fabrication process of the tailorable Er-GO-based MSCs, which connected in series can be used to drive small gadgets, such as a light-emitting diode (LED) and a mini-motor propeller. **Figure 4b** and **c** displays the morphology and structure of the Er-GO electrode, which exhibited a high areal specific capacitance (57.1 mF/cm^2) and an outstanding cycle stability (20,000 cycles with only 3.5% capacitance loss). Compared with conventional chemical reduction, the porous Er-GO layer can be homogeneously deposited on a conductive substrate and be used as the electrode material without any binder; besides, the production process of Er-GO can be conveniently scaled up, all of which made the electrochemical reduction routine more promising. CV curves of the MSC under different scan rates from 50 to 5000 mV/s in **Figure 4d** demonstrated the excellent rate capability of Er-GO-based MSCs, which can be attributed to the excellent electrical conductivity and porous structure of Er-GO itself. Furthermore, Er-GO-based MSCs exhibited excellent mechanical reliability, indicated by the little capacitance loss under pressure or bending, showing great potential in flexible, bendable, wearable, and even tailorable electronics.

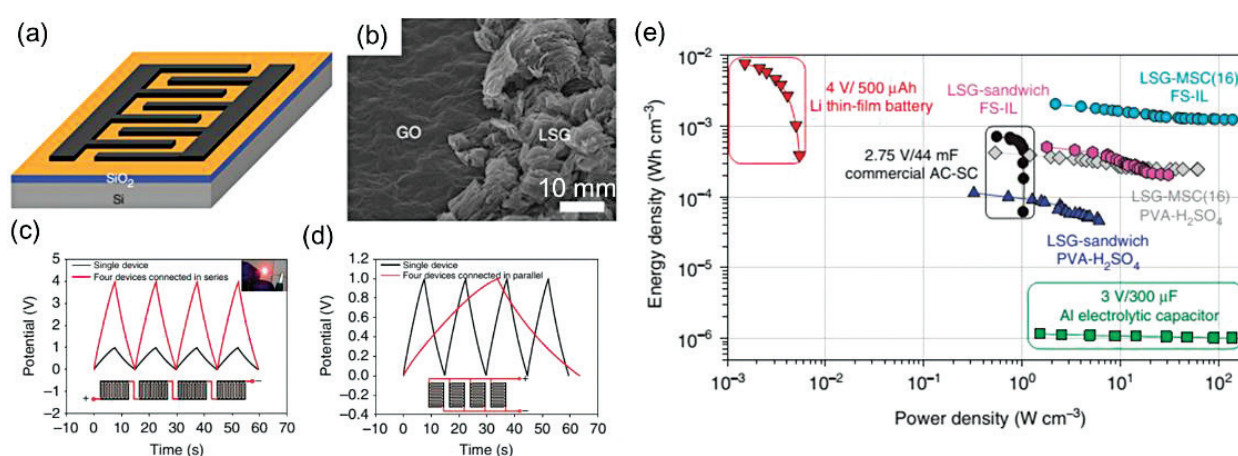


Figure 3. (a) Schematic illustration of r-GO-based MSCs on a chip, (b) SEM image showing the direct reduction and expansion of the GO film after exposure to the laser beam (scale bar is 10 mm), galvanostatic charge/discharge curves for four tandem microsupercapacitors connected (c) in series, and (d) in parallel, (e) energy and power densities of r-GO-based MSCs compared with commercially available energy-storage systems (Reproduced with permission from Ref. [38]).

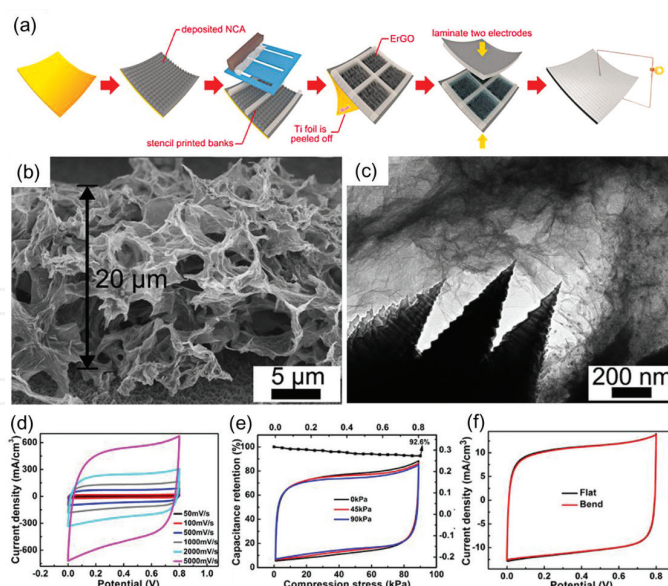


Figure 4. (a) Schematic illustration of the shape-tailorable r-GO-based ultra-high-rate supercapacitor (Regular nickel nanocone arrays (NCAs) deposited on a Ti substrate were used as current collector, and perpendicularly stencil-printed EVA glue was used as cofferdams, and Er-GO electrochemically deposited onto the NCAs was electrode material, and $\text{Na}_2\text{SO}_4/\text{PVA}$ gel was used as electrolyte), (b, c) SEM and TEM images of NCAs and Er-GO, (d) CV curves of the MSC under different scan rates from 50 to 5000 mV/s, (e) capacitance retention performance of the MSC under different compression strength, (f) CV curves of the MSC tested at 100 mV/s with and without bending (curvature radius: 1.7 cm) (Reproduced with permission from Ref. [39]).

Xie et al. in the same group also carried out a benchmark study of the state-of-the-art well-packaged ultrathin microsupercapacitor compared with commercial microsupercapacitor and aluminum electrolyte capacitor [40]. **Figure 5a** shows the fabrication process of the ultrathin and flexible MSCs using laser to complete the reduction and ablation of GO film to obtain patterned r-GO-based electrodes. **Figure 5b** gives the optical image of as-fabricated r-GO-based MSCs arrays, and **Figure 5c** demonstrates the porous structure of laser-processed r-GO film with a thickness of about 4 μm , providing more surface area and being beneficial to a high mobility of ions, both of which helped deliver high energy and power densities. The as-fabricated r-GO-based MSCs demonstrated great flexibility and bendability indicated by the almost same CV curves under different bending angles around a cylinder with a diameter of about 3 cm in **Figure 5d**. The Ragone plot in **Figure 5e** suggests that the energy density of this r-GO-based MSC with LiCl-PVA gel electrolyte achieved 0.98 mWh/cm^3 at the power density of 300 mW/cm^3 , which was almost three orders of magnitude higher than that of a commercial activated carbon supercapacitor. With the power density raised from 300 mW/cm^3 to 2000 mW/cm^3 , the energy density of this r-GO-based MSC had no significant degradation in capacitance, showing excellent rate performance. Furthermore, using the ionic liquid electrolyte, r-GO-based MSCs with a thickness of 18 μm can be fabricated with a maximum energy density up to 5.7 mWh/cm^3 at 830 mW/cm^3 , which can be comparable with lithium thin-film battery but with more than two orders of magnitude higher power density. However, their energy density was still not large enough for high-performance MSCs compared with those of Refs. [1, 38, 41]. The ultrathin thickness and foldability of as fabricated r-GO-based MSCs made it possible for them to be folded to fit in restricted spaces integrated with other

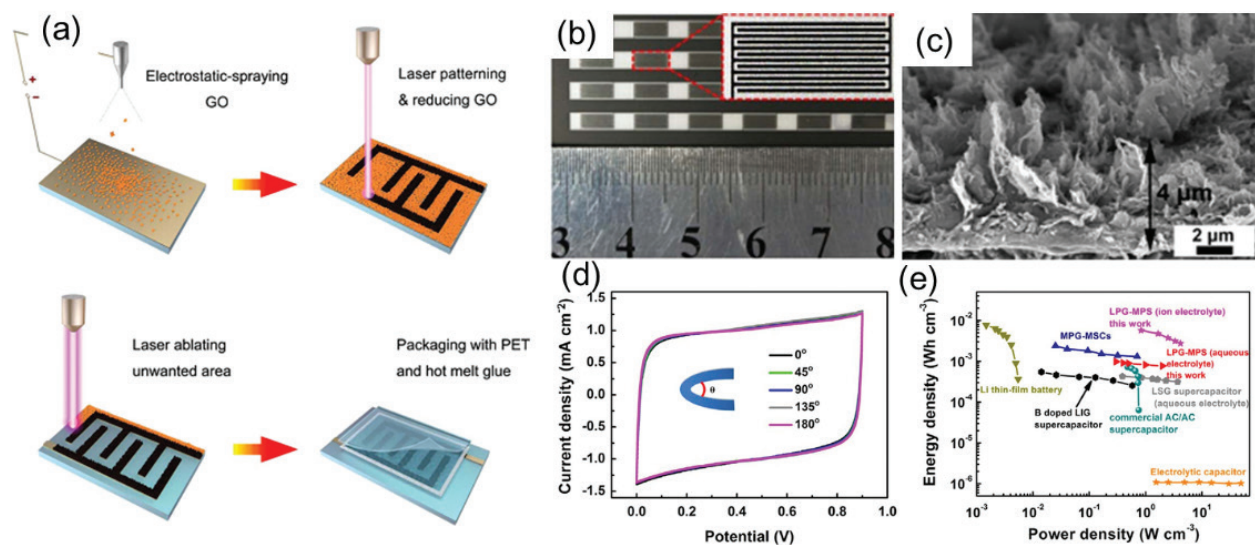


Figure 5. (a) Schematic illustration of ultrathin laser-processed r-GO-based MSCs (the PET substrate with a thickness of 6 μm sputtered with Ni layer (500 nm) was homogenously deposited with GO nanosheets by electrostatic spray deposition technique, and the reduction and ablation of GO film were completed by different power of laser treatment. Then, electrolyte was added and a thin PET film printed with cross-linkable PU cofferdams was used as the cover layer.), (b) photographic image of r-GO-based MSCs arrays (Inset is a single unit), (c) cross-view SEM image of laser processed r-GO with a height of about 4 μm , (d) CV curves of r-GO-based MSCs observed in different bending state, (e) Ragone plot of r-GO-based MSCs and some reported supercapacitors (Reproduced with permission from Ref. [40]).

components. Similarly, Meng et al. reported an integrated, flexible, and all-solid-state MSC technology with 3D microintegration capability [37]. They firstly embedded the entire electrical routing path and contact pads within the effective device area, utilizing the novel fabrication of through-via bottom electrodes. The entire device was successfully packaged with a solid-state electrolyte at the microscale ($720\ \mu\text{m} \times 720\ \mu\text{m} \times 50\ \mu\text{m}$) and has surface-mounted integration capability.

Wu et al. demonstrated r-GO-based in-plane interdigital MSCs with high power and energy densities on arbitrary substrates [1]. **Figure 6a** shows the fabrication process of the device. The resulting r-GO film had an electrical conductivity of 297 S/cm, and the as-fabricated r-GO-based MSCs showed the features of large-area uniformity, good transparency, and mechanical flexibility. The plot of the discharge current as a function of scan rate in **Figure 6b** demonstrated an enhanced electrochemical performance. A linear increase of discharge current can be observed up to 200 V/s, suggesting the ultrahigh power ability of r-GO-based MSCs. The as-fabricated r-GO-based MSCs can be operated at an ultrahigh rate up to 1000 V/s and showed an excellent capacitance. For example, an areal capacitance of 78.9 mF/cm² and a volumetric capacitance of 17.5 F/cm³ were obtained for the device at 10 mV/s in **Figure 6c**. The Ragone plot in **Figure 5e** suggests that the r-GO-based MSCs delivered a volumetric energy density of 2.5 mWh/cm³, which was an order of magnitude higher than that of the typical supercapacitors of activated carbon ($\leq 1\ \text{mWh/cm}^3$) and well comparable to that of lithium thin film batteries (10^{-3} – $10^{-2}\ \text{Wh/cm}^3$). Furthermore, the r-GO-based MSC manifested an ultrahigh power density of 495 W/cm³, which was 50 times higher than that of conventional

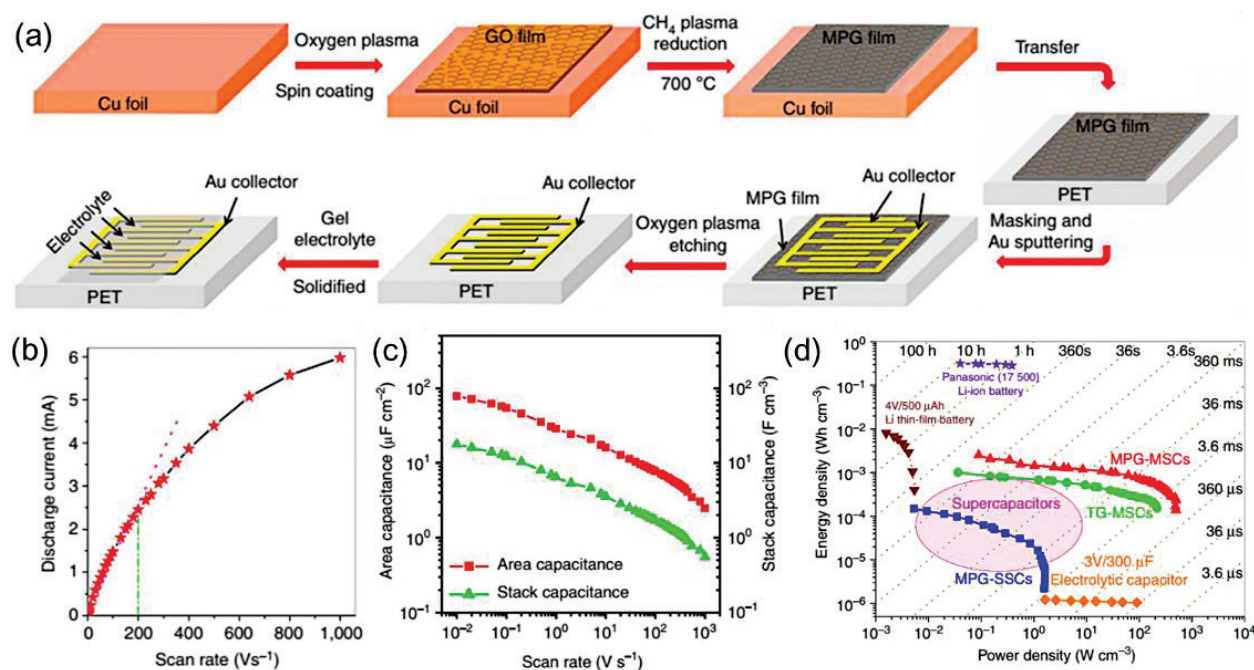


Figure 6. (a) Schematic illustration of the fabrication of flexible r-GO-based flexible MSCs (The fabrication process included a sequence of spin-coating of GO solution on Cu foil, CH₄ plasma reduction of GO film, transfer of r-GO film from the Cu foil to PET substrate, masking pattern and deposition of gold current collector, oxidative etching, drop casting of H₂SO₄/PVA gel electrolyte and solidification of gel electrolyte.), (b) a plot of the discharge current as a function of the scan rate (red star line) (linear dependence (magenta dot line) was observed up to at least 200 V/s (green dash dot line), suggesting the ultrahigh power ability of r-GO-based MSCs.), (c) areal capacitance and stack capacitance of r-GO-based MSCs, (d) the comparison of energy and power density of as fabricated MSGs with commercially applied electrolytic capacitors, lithium thin-film batteries, Panasonic Li-ion battery, and conventional supercapacitors (indicated by the pink region), demonstrating that the as-fabricated MSCs exhibited exceptional electrochemical energy storage with simultaneous ultrahigh energy density and power density (Reproduced with permission from Ref. [1]).

supercapacitors (even at a high energy density of 0.14 mWh/cm³) when discharged within an extremely short time (1 ms) and much higher than those in Refs. [38–40].

Wu et al. in the same group also described the development of large-area, highly uniform, ultrathin nitrogen and boron co-doped graphene (BNG) films for high-performance MSCs [41]. The BNG film was prepared using a layer-by-layer (LBL) assembly technique of anionic GO nanosheets and cationic poly-L-Lysine (PLL) as a nitrogen-containing precursor, followed by intercalation of H₃BO₃ within the layers and annealing treatment. Remarkably, BNG-MSCs allowed for operation at an ultrahigh scan rate of up to 2000 V/s, which was three orders of magnitude higher than that of conventional supercapacitors and represented superior value for high-power MSCs. The volumetric capacitance of BNG film for MSCs recorded at 10 mV/s was ~488 F/cm³, which can be attributed to the co-doping with dual heteroatoms. On one hand, the co-doping strategy created new electrochemically active moieties (e.g., B-N-C) with a synergistic effect that provides additional pseudocapacitance contribution, and on the other hand, the new binding environment of neighboring B and N atoms directly incorporated into the graphene lattice was favorable for improving the interface wettability of the electrode

with the electrolyte, resulting in a thickened electrochemical double layer. Furthermore, based on the volumetric capacitance and working voltage (1.0 V), the energy density and power density were calculated to be about 16.9 mWh/cm³ and 910 W/cm³, which was among best performances of the-state-of-art carbon-based MSCs.

Even significant progress has been achieved in the field of carbon-based MSCs in recent years, their application as energy storage devices is still limited due to their low energy density, which results in a high cost per kilowatt-hour, i.e., around 20,000\$/kWh, significantly higher than those of well-established storage technologies (such as batteries) [42]. One direct way to lower their cost is to find suitable electrode materials with high energy storage capability without any damage to their power handling ability, for example, the MSCs based on graphene and MnO₂ hybrid materials demonstrated a two times higher energy density than that of initial pure graphene due to the Faradaic pseudocapacitance effect of MnO₂ [43]. Another way is to use fabrication methods compatible with efficient large-scale production throughout the fabrication process of MSCs, including preparation of electrode materials, fabrication of electrodes, and assembly of electrodes, electrolyte, and/or separator as well as their packaging process, for instance, combining with low-cost printing technology during electrode fabrication process can greatly lower the total cost [44].

4. Conclusions

In summary, this chapter reviews the recent research advances of r-GO as a promising electrode material for miniaturized MSCs. R-GO exhibited many advantages such as excellent rate capability, high power density, long lifetime, facile production in large scale and low costs. However, further enhancement in performance characteristics and functionality of r-GO-based miniaturized MSCs need more attentions before this promising technology may be adopted by industry. Combined with novel film-fabrication, patterning, and packaging techniques, miniaturized r-GO-based MSCs with superior capability to be integrated with other components on chip and system levels can be developed due to their ultrathin thickness, flexibility, bendability, foldability, and even tailorability. The examples given in this chapter also discussed about their merits and limitations, we expect that they may give elicitation for developing advanced techniques for the fabrication of high-performance and multifunction miniaturized r-GO-based MSCs in the near future.

Acknowledgements

The authors acknowledge the financial support from National Nature Science Foundation of China Project Nos. 51578310 & 51607102; China Postdoctoral Science Foundation No. 2016M601017, Guangdong Province Science and Technology Department Project Nos. 2014B090915002 & 2015A030306010, and Nanshan District "Rising Stars" Project No. KC2014JSQN0010A.

Author details

Zhi Jiang, Yang Wang and Cheng Yang*

*Address all correspondence to: yang.cheng@sz.tsinghua.edu.cn

Division of Energy & Environment, Graduate School at Shenzhen, Tsinghua University, Shenzhen City, Guangdong Province, China

References

- [1] Wu Z S, Parvez K, Feng X, Mullen K: Graphene-based in-plane micro-supercapacitors with high power and energy densities. *Nature Communications*. 2013;4:2487. DOI: 10.1038/ncomms3487
- [2] Wu Z S, Feng X, Cheng H M: Recent advances in graphene-based planar micro-supercapacitors for on-chip energy storage. *National Science Review*. 2013;1:277–292. DOI: 10.1093/nsr/nwt003
- [3] Wen F, Hao C, Xiang J, Wang L, Hou H, Su Z, Hu W, Liu Z: Enhanced laser scribed flexible graphene-based micro-supercapacitor performance with reduction of carbon nanotubes diameter. *Carbon*. 2014;75:236–243. DOI: 10.1016/j.carbon.2014.03.058
- [4] Zhu J, Yang D, Yin Z, Yan Q, Zhang H: Graphene and graphene-based materials for energy storage applications. *Small*. 2014;10:3480–3498. DOI: 10.1002/smll.201303202
- [5] Zhang Q, Scrafford K, Li M, Cao Z, Xia Z, Ajayan P M, Wei B: Anomalous capacitive behaviors of graphene oxide based solid-state supercapacitors. *Nano Letter*. 2014;14:1938–1943. DOI: 10.1021/nl4047784
- [6] Kim B C, Hong J-Y, Wallace G G, Park H S: Recent progress in flexible electrochemical capacitors: electrode materials, device configuration, and functions. *Advanced Energy Materials*. 2015;5:1500959. DOI: 10.1002/aenm.201500959
- [7] Kuila T, Mishra A K, Khanra P, Kim N H, Lee J H: Recent advances in the efficient reduction of graphene oxide and its application as energy storage electrode materials. *Nanoscale*. 2013;5:52–71. DOI: 10.1039/c2nr32703a
- [8] Singh R K, Kumar R, Singh D P: Graphene oxide: strategies for synthesis, reduction and frontier applications. *RSC Advances*. 2016;6:64993–65011. DOI: 10.1039/c6ra07626b
- [9] Gao X, Joonkyung J, Shigeru N: Hydrazine and thermal reduction of graphene oxide reaction mechanisms, product structures, and reaction design. *Journal of Physics Chemistry C*. 2010;114:832–842. DOI: 10.1021/jp909284g
- [10] Ren P G, Yan D X, Ji X, Chen T, Li Z M: Temperature dependence of graphene oxide reduced by hydrazine hydrate. *Nanotechnology*. 2011;22:055705. DOI: 10.1088/0957-4484/22/5/055705

- [11] Pei S, Cheng H M: The reduction of graphene oxide. *Carbon*. 2012;50:3210–3228. DOI: 10.1016/j.carbon.2011.11.010
- [12] Zhou X, Zhang J, Wu H, Yang H, Zhang J, Guo S: Reducing graphene oxide via hydroxylamine: a simple and efficient route to graphene. *The Journal of Physical Chemistry C*. 2011;115:11957–11961. DOI: 10.1021/jp202575j
- [13] Stankovich S, Dikin D A, Dommett G H, Kohlhaas K M, Zimney E J, Stach E A, Piner R D, Nguyen S T, Ruoff R S: Graphene-based composite materials. *Nature*. 2006;442:282–286. DOI: 10.1038/nature04969
- [14] Pham T A, Kim J S, Kim J S, Jeong Y T: One-step reduction of graphene oxide with l-glutathione. *Colloids and Surfaces A: Physicochemical and Engineering Aspects*. 2011;384:543–548. DOI: 10.1016/j.colsurfa.2011.05.019
- [15] Chen D, Li L, Guo L: An environment-friendly preparation of reduced graphene oxide nanosheets via amino acid. *Nanotechnology*. 2011;22:325601. DOI: 10.1088/0957-4484/22/32/325601
- [16] Jiang B, Tian C, Wang L, Sun L, Chen C, Nong X, Qiao Y, Fu H: Highly concentrated, stable nitrogen-doped graphene for supercapacitors: simultaneous doping and reduction. *Applied Surface Science*. 2012;258:3438–3443. DOI: 10.1016/j.apsusc.2011.11.091
- [17] Li X, Wang H, Robinson J T, Sanchez H, Diankov G, Dai H: Simultaneous nitrogen doping and reduction of graphene oxide. *Journal of American Chemistry Society*. 2009;131:15939–15944. DOI: 10.1021/ja907098f
- [18] Thakur S, Karak N: Alternative methods and nature-based reagents for the reduction of graphene oxide: a review. *Carbon*. 2015;94:224–242. DOI: 10.1016/j.carbon.2015.06.030
- [19] Schniepp H C, Li J L, McAllister M J, Sai H, Herrera-Alonso M, Adamson D H, Prud'homme R K, Car R, Saville D A, Aksay I A: Functionalized single graphene sheets derived from splitting graphite oxide. *The Journal of Physical Chemistry B*. 2006;110:8535–8539. DOI: 10.1021/jp060936f
- [20] Vallés C, David Núñez J, Benito A M, Maser W K: Flexible conductive graphene paper obtained by direct and gentle annealing of graphene oxide paper. *Carbon*. 2012;50:835–844. DOI: 10.1016/j.carbon.2011.09.042
- [21] Mattevi C, Eda G, Agnoli S, Miller S, Mkhoyan K A, Celik O, Mastrogiiovanni D, Granozzi G, Garfunkel E, Chhowalla M: Evolution of electrical, chemical, and structural properties of transparent and conducting chemically derived graphene thin films. *Advanced Functional Materials*. 2009;19:2577–2583. DOI: 10.1002/adfm.200900166
- [22] Li Y, Sheng K, Yuan W, Shi G: A high-performance flexible fibre-shaped electrochemical capacitor based on electrochemically reduced graphene oxide. *Chemical Communications*. 2013;49:291–293. DOI: 10.1039/c2cc37396c
- [23] Yang J, Gunasekaran S: Electrochemically reduced graphene oxide sheets for use in high performance supercapacitors. *Carbon*. 2013;51:36–44. DOI: 10.1016/j.carbon.2012.08.003

- [24] Chen K, Chen L, Chen Y, Bai H, Li L: Three-dimensional porous graphene-based composite materials: electrochemical synthesis and application. *Journal of Materials Chemistry*. 2012;22:20968. DOI: 10.1039/c2jm34816k
- [25] Sheng K, Sun Y, Li C, Yuan W, Shi G: Ultrahigh-rate supercapacitors based on electrochemically reduced graphene oxide for ac line-filtering. *Scientific Reports*. 2012;2:247. DOI: 10.1038/srep00247
- [26] Shao Y, Wang J, Engelhard M, Wang C, Lin Y: Facile and controllable electrochemical reduction of graphene oxide and its applications. *Journal of Materials Chemistry*. 2010;20:743–748. DOI: 10.1039/b917975e
- [27] Sokolov D A, Rouleau C M, Geohegan D B, Orlando T M: Excimer laser reduction and patterning of graphite oxide. *Carbon*. 2013;53:81–89. DOI: 10.1016/j.carbon.2012.10.034
- [28] Huang L, Liu Y, Ji L C, Xie Y Q, Wang T, Shi W-Z: Pulsed laser assisted reduction of graphene oxide. *Carbon*. 2011;49:2431–2436. DOI: 10.1016/j.carbon.2011.01.067
- [29] Moussa S, Atkinson G, SamyEl-Shall M, Shehata A, AbouZeid K M, Mohamed M B: Laser assisted photocatalytic reduction of metal ions by graphene oxide. *Journal of Materials Chemistry*. 2011;21:9608. DOI: 10.1039/c1jm11228g
- [30] Zhang Y, Guo L, Wei S, He Y, Xia H, Chen Q, Sun H-B, Xiao F-S: Direct imprinting of microcircuits on graphene oxides film by femtosecond laser reduction. *Nano Today*. 2010;5:15–20. DOI: 10.1016/j.nantod.2009.12.009
- [31] Abdelsayed V, Moussa S, Hassan H M, Aluri H S, Collinson M M, El-Shall M S: Photothermal deoxygenation of graphite oxide with laser excitation in solution and graphene-aided increase in water temperature. *The Journal of Physical Chemistry Letters*. 2010;1:2804–2809. DOI: 10.1021/jz1011143
- [32] Kaplan A, Lenner M, Palmer R E: Emission of ions and charged clusters due to impulsive Coulomb explosion in ultrafast laser ablation of graphite. *Physical Review B*. 2007;76:073401. DOI: 10.1103/PhysRevB.76.073401
- [33] Lenner M, Kaplan A, Huchon C, Palmer R E: Ultrafast laser ablation of graphite. *Physical Review B*. 2009;79:184105. DOI: 10.1103/PhysRevB.79.184105
- [34] Carbone F, Baum P, Rudolf P, Zewail A H: Structural preablation dynamics of graphite observed by ultrafast electron crystallography. *Physical Review Letters*. 2008;100:035501. DOI: 10.1103/PhysRevLett.100.035501
- [35] Gao W, Singh N, Song L, Liu Z, Reddy A L, Ci L, Vajtai R, Zhang Q, Wei B, Ajayan P M: Direct laser writing of micro-supercapacitors on hydrated graphite oxide films. *Nature Nanotechnology*. 2011;6:496–500. DOI: 10.1038/nnano.2011.110
- [36] El-Kady M F, Strong V, Dubin S, Kaner R B. Laser scribing of high-performance and flexible graphene-based electrochemical capacitors. *Science*. 2012;335:1226–1230. DOI: 10.1126/science.1216744
- [37] Meng C, Maeng J, John S W M, Irazoqui P P: Ultrasmall integrated 3D micro-supercapacitors solve energy storage for miniature devices. *Advanced Energy Materials*. 2014;4:1301269. DOI: 10.1002/aenm.201301269

- [38] El-Kady M F, Kaner R B: Scalable fabrication of high-power graphene micro-supercapacitors for flexible and on-chip energy storage. *Nature Communications*. 2013;4:1475. DOI: 10.1038/ncomms2446
- [39] Xie B, Yang C, Zhang Z, Zou P, Lin Z, Shi G, Yang Q, Kang F, Wong C-P: Shape-tailorable graphene-based ultrahigh rate supercapacitor for wearable electronics. *ACS Nano*. 2015;9:5636–5645. DOI: 10.1021/acsnano.5b00899
- [40] Xie B, Wang Y, Lai W, Lin W, Lin Z, Zhang Z, Zou P, Xu Y, Zhou S, Yang C, Kang F, Wong C-P: Laser-processed graphene based micro-supercapacitors for ultrathin, rollable, compact and designable energy storage components. *Nano Energy*. 2016;26:276–285. DOI: 10.1016/j.nanoen.2016.04.045
- [41] Wu Z S, Parvez K, Winter A, Vieker H, Liu X, Han S, Turchanin A, Feng X, Mullen K: Layer-by-layer assembled heteroatom-doped graphene films with ultrahigh volumetric capacitance and rate capability for micro-supercapacitors. *Advanced Materials*. 2014;26:4552–4558. DOI: 10.1002/adma.201401228
- [42] Hadjipaschalis I, Poullikkas A, Efthimiou V: Overview of current and future energy storage technologies for electric power applications. *Renewable and Sustainable Energy Reviews*. 2009;13:1513–1522. DOI: 10.1016/j.rser.2008.09.028
- [43] Liu W W, Feng Y Q, Yan X B, Chen J T, Xue Q J: Superior micro-supercapacitors based on graphene quantum dots. *Advanced Functional Materials*. 2013;23:4111–4122. DOI: 10.1002/adfm.201203771
- [44] Fukuda K, Minamiki T, Minami T, Watanabe M, Fukuda T, Kumaki D, Tokito S: Printed Organic Transistors with Uniform Electrical Performance and Their Application to Amplifiers in Biosensors. *Advanced Electronic Materials*. 2015;1:1400052. DOI: 10.1002/aelm.201400052

IntechOpen